VISUALIZATION OF TWO-PHASE GAS-LIQUID FLOW REGIMES IN HORIZONTAL AND SLIGHTLY-INCLINED CIRCULAR TUBES

Lívia Alves de Oliveira, livia@lasme.coppe.ufrj.br
Nuclear Engineering Institute, Brazilian Nuclear Energy Commission (CNEN) CP 68550, Rio de Janeiro, $21945-970$, Brazil
Jurandyr S. Cunha Filho, cunhafilho@lasme.coppe.ufrj.br
Nuclear Engineering Program, COPPE, Universidade Federal do Rio de Janeiro. CP 68509, Rio de Janeiro, $21945-970$, Brazil
José Luiz Horácio Faccini, faccini@ien.gov.br
Nuclear Engineering Institute, Brazilian Nuclear Energy Commission (CNEN) CP 68550, Rio de Janeiro, $21945-970$, Brazil
Jian Su, sujian@lasme.coppe.ufrj.br
Nuclear Engineering Program, COPPE, Universidade Federal do Rio de Janeiro. CP 68509, Rio de Janeiro, $21945-970$, Brazil

Abstract. *In this paper a flow visualization study was performed for two-phase gas-liquid flow in horizontal and slightly-inclined tubes. The test section consists of a 2.54 cm inner diameter stainless steel circular tube, followed by a transparent acrylic tube with the same inner diameter. The working fluids were air and water, with liquid superficial velocities ranging from* 0.11 *to* 3.28 m/s *and gas superficial velocities ranging from* 0.27 *to* 5.48 m/s*. Flow visualization was executed for upward flow at* $5°$ *and* $10°$ *and downward flow at* $2.5°$*,* $5°$ *and* $10°$*, as well as for horizontal flow. The visualization technique consists of a high-speed digital camera that records images at rates of* 125 *and* 250 *frames per second of a concurrent air-water mixture through a transparent part of the tube. From the obtained images, the flow regimes were identified (except for annular flow), observing the effect of inclination angles on flow regime transition boundaries. Finally, the experimental results were compared with empirical and theorical flow pattern maps available in literature.*

Keywords: *multiphase flow, flow patterns, air-water flow, flow visualization*

1. INTRODUCTION

Multiphase flow is an important field of study since its presence is constant in many industrial and natural processes. For example, clouds are drops of liquid moving (dispersed in gas phase); oil, gas and water coexist inside porous rocks; heat transfer by boiling is of great importance for electrical generation; primary refrigeration circuit of nuclear reactors needs constant control of the gas-liquid two-phase flow parameters, among other occurrences.

The simplest and most common approach to study two-phase gas-liquid flow patterns is to visualize and observe the two-phase flow through a transparent section window. The visualization technique by photographing at high speed has been widely applied in gas-liquid two-phase flow studies, for a simple visual observation of flow patterns or for the measurements of relevant flow parameters. Bui-Dinh and Choi (2001) developed a method for the instantaneous bubble rise velocity measurements in vertical upward two-phase flow regimes using digital image processing algorithms. Zaruba et al. (2005) experimentally investigated a bubble column, using a high-speed video camera to measure the individual bubble displacements and their velocities. Mayor et al. (2007) analysed the uncertainty associated with an imaging technique used to measure relevant parameters (such as bubble length and velocity) of a slug flow. The same experimental approach appears many times associated with others for two-phase flow measurements: Morala et al. (1984) employed this technique with an ultrasonic one, Fairholm et al. (1991) and Mishima et al. (1997) applied it in association with neutrongraphy. Fossa et al. (2003) and Woods et al. (2006) employed it with impedance and conductance, respectively. Recently Supa-Amornkul et al. (2005) used a commercial computational fluid dynamics (CFD) code to model the results obtained from a flow visualization study in a CANDU reactor. As a non-invasive method, the visualization technique allows the analyzed system to be free of any external interference.

The objective of the present research is to perform a flow visualization study of two-phase gas-liquid flow in horizontal and slightly inclined circular tubes, and compare the observed flow patterns with availabe empirical and theoretical flow pattern maps. The paper is organized as follows: in Section 2. the two-phase flow test section is described, as well as the flow visualization technique applied; in Section 3. the Mandhane et al. (1974) and the Taitel and Dukler (1976) flow regime maps are presented; the results of flow visualization and comparison with the Mandhane et al. (1974) and the Taitel and Dukler (1976) maps are presented in Section 4.

2. EXPERIMENTAL SET UP

A schematic diagram and a descripition of the experimental facilities are given as follows: the inclined two-phase flow test section controls the flow conditions to achieve the desired flow pattern and the visualization system records the flow pattern visual observations.

2.1 Two-Phase Flow Test Section

The inclined two-phase flow test section consists of a water flow loop, a feed compressed air system, an airwater mixer, an inclined pipe test section and a separation air atmospheric tank, as shown in 1. A schematic diagram of the experimental test section appears in Figure 1. The inclined pipe is a $6\ m$ long stainless steel 316 pipe with inner diameter of $1\ in$, connected by flanges in a transparent $1.8\ m$ long acrylic pipe of with the same inner diameter. Distilled water is circulating through the mixer, coming from an existing single-phase water loop which is equipped with a centrifugal pump and a metering ring. Air is injected in the radial direction into the mixer by a compressor through a flow line equipped with appropriate air instrumentation. The air flow rate is measured by two rotameters (uncertainty $\pm\ 3\%$). A thermocouple is installed in the region of the air injector to measure the air temperature. The water flow rate is measured by a turbine flowmeter (uncertainty $\pm\ 0.5\%$) or a rotameter according to the flow rate range. The air-water mixture goes out from the mixer and travels through a stainless steel tube along its length until the transparent acrylic pipe where it can be visually observed. The two-phase flow in the pipes is operated at pressures and temperatures close to atmospheric conditions. Measurements were executed in the acrylic pipe.

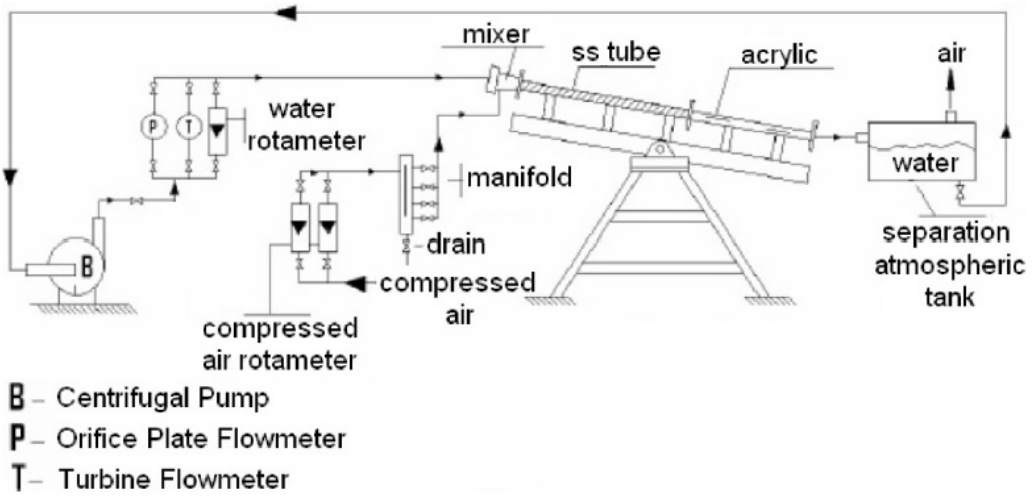

Figure 1. Two-phase flow test section.

2.2 Visualization System

The visualization system is formed by a monochrome digital high-speed camera equipped with a CCD sensor (maximum resolution 480 x 420 pixels), zoom lenses, a PCI controller board of 12 bits, an acquisition and image analysis program and a computer, as shown in Figure 2. The system is able to catch images at a rate from 50 up to 8000 frames per second. The frequency range from 125 to 250 frames per second was found to be adequate for the measurements and was used in all experiments reported in this paper. The sequence of images displayed on the computer monitor were stored in a computer file, retrieved and replayed afterwards to analyze the flow motion sequence in detail. The set of discrete pictures was saved as a series of 512 greyscale avi images with a spatial resolution of 480x420 pixels. The lighting is provided by two projectors placed in front of and above the acrylic tube.

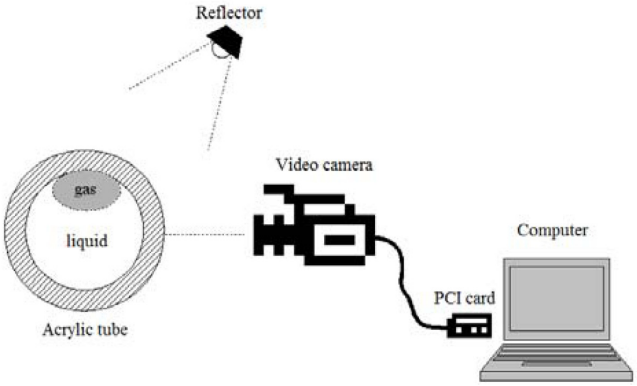

Figure 2. Visualization system.

3. FLOW REGIMES MAPS

In literature, many different types of flow regimes maps have been developed for the prediction of flow patterns. Empirical maps were developed from experimental data, like Baker (1954), Begss and Brill (1973), Mandhane et al. (1974) presented different empirical maps. Taitel and Dukler (1976) developed a mechanistic approach.

The most popular regimes in multiphase flow are classified according to the shape and distribution of the interfaces in way the phases are disposed inside the tube. The observed flow patterns, in horizontal flow, are: bubbly flow, plug flow, stratified flow (smooth and wavy), slug flow and annular flow. These are the most common designation for flow patterns that appear in literature and are shown in Figure 3.

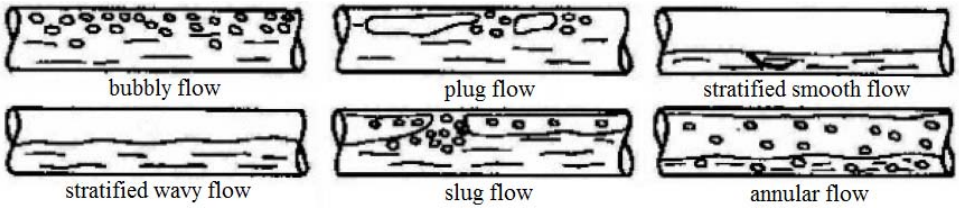

Figure 3. Horizontal flow patterns.

Flow regimes maps are developed to predict flow regimes from certain parameters and consequently give some information about pressure gradient, liquid hold-up, etc. In these maps, different flow patterns are presented as regions limited by transition lines. These lines represent the change from one flow regime to another due to variations in a certain flow parameter.

Empirical maps are developed from experimental data, in wich the coordinate axis consist of dimensionless groups, phases superficial velocities, mass or momentum flux. A large number of data about the flow patterns can be found in literature, mainly air-water. There is a necessity to generalize the available data to cover a wide range of parameters, like fluid properties, pipe dimensions and operational conditions. The precision in determination of the transition lines depends on the numbers of experiments studied and the parameters used on the map coordinate axis because of the transient interfaces in two-phase flow. The different classifications of the flow patterns and the dissimilar terms used to designate them by different authors make the study and comparison between the transition lines more difficult.

The theoretical maps are developed from models that mathematically express the mechanisms for patterns transition, based on physical concepts, and are fully predictive in that no flow regime data is used in their development.

The Mandhane et al. (1974) map was selected as empirical and the Taitel and Dukler (1976) map was selected as theoretical to be analysed because of their good acceptance and use.

3.1 Mandhane et al. (1974) Map

The flow regime map proposed by Mandhane et al. (1974) shows a flow regime correlation (an extension of the study of Govier and Aziz (1972)) developed in agreement with almost six thousand horizontal flow patterns observations. This comprehensive experimental data bank represents a very wide range of parameters as is shown in Table 1. The map has been well accepted and used by many researchers. An important observation is that the majority of the data was obtained for an air-water flow in pipes of 0.5 to 6.1 in in order to simplify the analysis, resulting in transition boundaries substantially affected by these systems. The air-water system parameters used are shown in Table 2. Corrections were applied for other fluidt's physics properties to obtain the large range of parameters values.

Table 1. Range of parameter values for data used by Mandhane et al. (1974).

Parameter	Values
Inside pipe diameter (D)	0.5-6.1 in
Liquid phase density (ρ_L)	44.0-63.0 $lb./ft^3$
Gas phase density (ρ_G)	0.05-3.15 $lb./ft^3$
Liquid phase viscosity (μ_L)	0.30-90.0 centipoise
Gas phase viscosity (μ_G)	0.010-0.022 centipoise
Surface tension (σ)	24.0-103.0 dynes/cm
Superficial liquid velocity (U_{LS})	0.003-24.0 ft./s
Superficial gas velocity (U_{GS})	0.14-560 ft./s

Table 2. Range of parameter values used as criteria for air-water system.

Parameter	Values
Liquid phase density (ρ_L)	60.0-65.0 $lb./ft^3$
Gas phase density (ρ_G)	0.065-0.090 $lb./ft^3$
Liquid phase viscosity (μ_L)	0.75-1.1 centipoise
Gas phase viscosity (μ_G)	0.017-0.02 centipoise
Surface tension (σ)	69.0-73.0 dynes/cm

The Mandhane et al. (1974) flow regime map associates the gas and liquid superficial velocities through the correlation algorithm developed in their work as is shown in Figure 4.

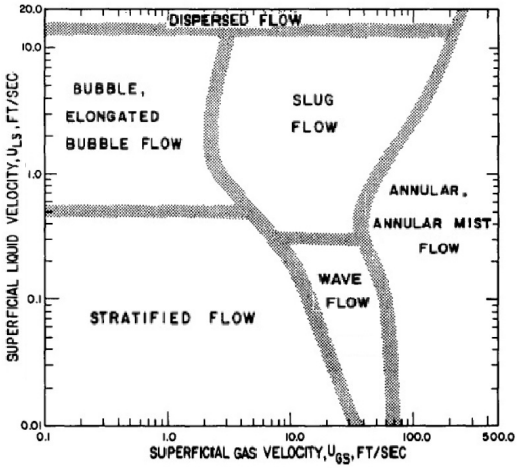

Figure 4. Horizontal flow patterns.

3.2 Taitel and Dukler (1976) Map

Taitel and Dukler (1976) associated the following variables in which flow regime transitions take place: gas and liquid mass flow rates, properties of the fluids, pipe diameter and angle of inclination to the horizontal. Their analysis considers the conditions for transition between five basic flow regimes: smooth stratified, wavy stratified, intermittent (slug and plug), annular with dispersed liquid and dispersed bubble. The transitions analysis starts from the condition of stratified flow and then other mechanisms to achieve the other regimes are discussed. A visual observation of the considered system is shown in Figure 5. The momentum balance on each phase (eq. 1 and eq. 2) provides a relation for the pressure drop in both phases (eq. 3) for the smooth, equilibrium stratified flow.

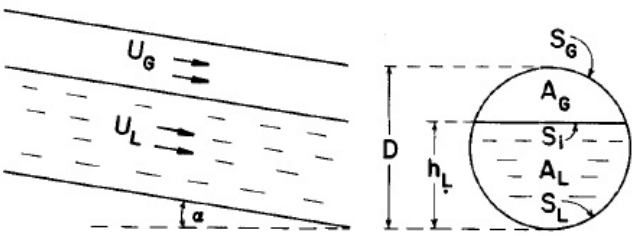

Figure 5. Equilibrium stratified flow.

$$-A_L\left(\frac{dP}{dx}\right) - \tau_{WL}S_L + \tau_{Wi}S_i + \rho_L g A_L \sin\alpha = 0, \tag{1}$$

$$-A_G\left(\frac{dP}{dx}\right) - \tau_{WG}S_G - \tau_{Wi}S_i + \rho_G g A_G \sin\alpha = 0, \tag{2}$$

$$\tau_{WG}\frac{S_G}{A_G} - \tau_{WL}\frac{S_L}{A_L} + \tau_{Wi}S_i\left(\frac{1}{A_L} + \frac{1}{A_G}\right) + (\rho_L - \rho_G)g\sin\alpha = 0. \tag{3}$$

From a dimensionless form of the pressure drop equation (eq. 3), two dimensionless groups are obtained: X and Y, represented in eq. 4 and eq. 5 respectively.

$$X = \sqrt{\frac{\frac{4C_L}{D}\left(\frac{U_{LS}D\rho_L}{\mu_L}\right)^{-n}\frac{\rho_L(U_{LS})^2}{2}}{\frac{4C_G}{D}\left(\frac{U_{GS}D\rho_G}{\mu_G}\right)^{-m}\frac{\rho_G(U_{GS})^2}{2}}} = \sqrt{\frac{|(dP/dx)_{LS}|}{|(dP/dx)_{GS}|}}, \tag{4}$$

$$Y = \frac{(\rho_L - \rho_G)\, g \sin\alpha}{\frac{4C_G}{D}\left(\frac{U_{GS}D\rho_G}{\mu_G}\right)^{-m}\frac{\rho_G(U_{GS})^2}{2}} = \frac{(\rho_L - \rho_G)\, g \sin\alpha}{|(dP/dx)_{GS}|}. \tag{5}$$

There are three dimensioless groups associated with the flow regime transitions: F group (eq. 6) is for the transition between stratified and intermittent or annular with dispersed liquid regimes and is also used for the transition between intermittent and annular with dispersed liquid with a constant value of X, when h_L/D = 0.5 ; K group (eq. 7) is for the transition between stratified smooth and stratified wavy regimes; T (eq. 8)is for the transition between intermittent and dispersed bubble regimes.

$$F = U_{GS}\sqrt{\frac{\rho_G}{gD\,(\rho_L - \rho_G)\cos\alpha}}, \tag{6}$$

$$K = \sqrt{\frac{\rho_G\,(U_{GS})^2}{gD\,(\rho_L - \rho_G)\cos\alpha}\frac{\rho_L U_{LS} D}{\mu_L}}, \tag{7}$$

$$T = \sqrt{\frac{\frac{4C_L}{D}\left(\frac{U_{LS}D\rho_L}{\mu_L}\right)^{-n}\frac{\rho_L(U_{LS})^2}{2}}{(\rho_L - \rho_G)\, g\cos\alpha}}. \tag{8}$$

These dimensionless groups representing the transition lines are plotted in terms of the superficial phases velocities, as shown for the horizontal flow in Figure 6.

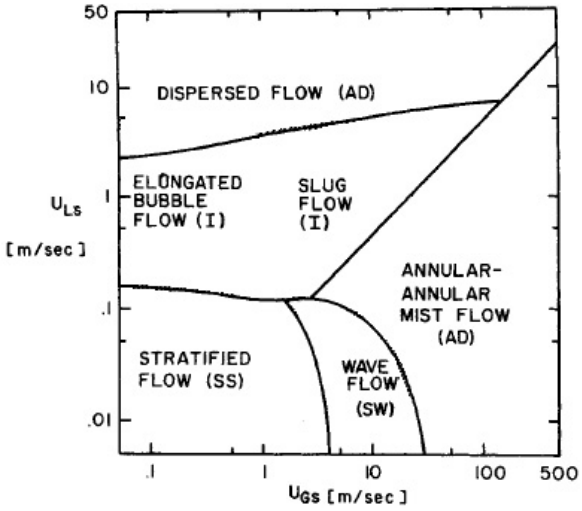

Figure 6. Taitel and Dukler (1976) map for horizontal flow, air-water, D = 2.5 cm.

4. RESULTS

The Mandhane et al. (1974) experimental correlation algorithm and Taitel and Dukler (1976) model were implemented in Wolfram *Mathematica 7.0* software to provide the following maps. For Taitel and Dukler (1976) model, the utilized coefficients were $C_G = C_L$ = 0.046 and n = m = 0.2 in order to provide turbulent flow for both phases (laminar flow of the liquid was not used because of its little effect on the result). The laboratory conditions, in terms of fluid properties and line size, simulated in the Taitel and Dukler (1976) model are listed in Table 3.

Experiments were performed for stratified, intermittent and bubbly flow, with liquid superficial velocities ranging from 0.11 to $3.28\ m/s$ and gas superficial velocities ranging from 0.27 to $5.48\ m/s$. The annular and stratified flows, in some cases, were not obtained because of the pump and compressed air system operational limits.

Table 3. Laboratory conditions.

Parameter	Values
Inside pipe diameter (D)	1"
Liquid phase density (ρ_L)	998.2 kg/m^3
Gas phase density (ρ_G)	1.204 kg/m^3
Liquid phase viscosity (μ_L)	$1.005\text{x}10^{-3}$ Pa.s
Gas phase viscosity (μ_G)	$1.81\text{x}10^{-6}$ Pa.s
Angles of inclination (α)	$0°$,$-5°$,$-10°$,$+2.5°$,$+5°$

4.1 α = $0°$ (horizontal flow)

For horizontal flow, 31 experimental points were obtained and compared with Mandhane et al. (1974) and Taitel and Dukler (1976) maps as shown in Figure 7. There is a very satisfactory agreement in both maps concerning the significant curves trends and their absolute locations. It is also observed a good agreement with the experimental data, except for a few dispersed bubble flow points.

Mandhane et al. (1974) discussed the difficulty of many maps to correctly predict the dispersed bubble regime by comparing them with the experimental data bank he used.

The nomenclature used in Figure 7 corresponds to Mandhane et al. (1974) classification, where the elongated bubble and slug flows represent different kinds of intermittent flow.

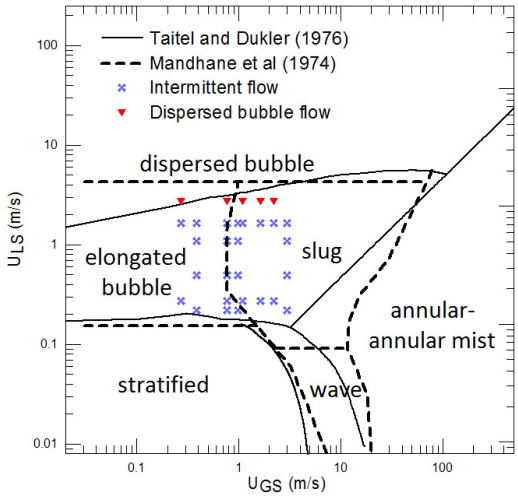

Figure 7. Comparison of the experimental data with Mandhane et al. (1974) and Taitel and Dukler (1976) maps for horizontal flow.

4.2 α = $-5°$ (upward flow)

For upward flow at $5°$, 33 experimental points were obtained and compared with Taitel and Dukler (1976) map as shown in Figure 8. Again, it is observed a good agreement of the experimental data with the map.

As noted for Taitel and Dukler (1976), the upward inclination causes intermittent flows to take place over a much wider range of flow conditions and the stratified flow region shrinks substantially. This happens because of gravity effects that makes the stability of stratified flow more difficult. As appears in Figure 8, these very strict conditions to achieve stratified flow could not be reproduced in laboratory.

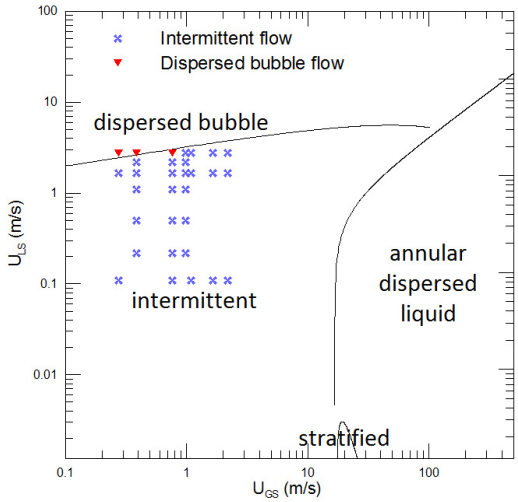

Figure 8. Comparison of the experimental data with Taitel and Dukler (1976) map for upward flow at $5°$.

4.3 $\alpha = -10°$ (upward flow)

For upward flow at $10°$, 35 experimental points were obtained and compared with Taitel and Dukler (1976) map as shown in Figure 9. Again, it is observed a good agreement of the experimental data with the map.

For this higher upward angle there were no conditions to reach the stratified flow in laboratory and even with very low gas rates it does not appear in the map.

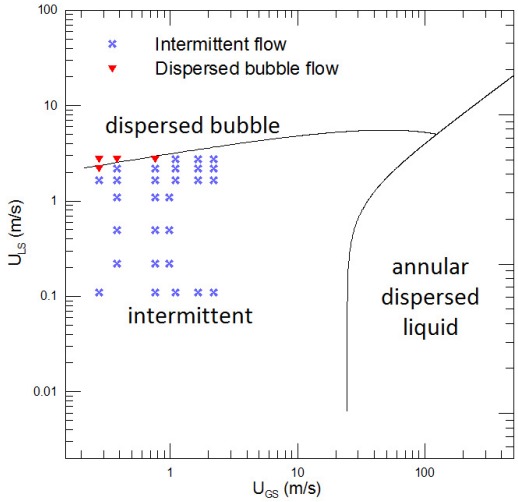

Figure 9. Comparison of the experimental data with Taitel and Dukler (1976) map for upward flow at $10°$.

4.4 $\alpha = +2.5°$ (downward flow)

For downward flow at $2.5°$, 28 experimental points were obtained and compared with Taitel and Dukler (1976) map as shown in Figure 10. Again, it is observed a good agreement of the experimental data with the map, except for a single intermittent flow point that seems as a transition situation with very elongated bubbles.

As noted for Taitel and Dukler (1976), the downward inclination causes the inverse effect of upward inclinations: the stratified region is bigger and the intermittent region is smaller. The stratified flow stability occurs since the downward inclination causes the liquid to move more rapidly, in a lower level and in a way that requires higher gas and liquid rates to begin the transition from stratified flow.

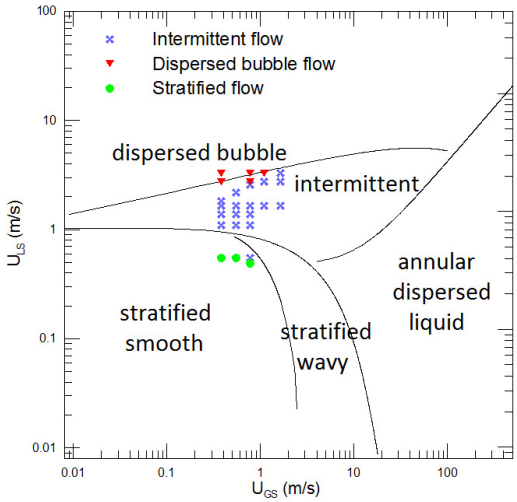

Figure 10. Comparison of the experimental data with Taitel and Dukler (1976) map for downward flow at $2.5°$.

4.5 $\alpha = +5°$ (downward flow)

For downward flow at $5°$, 84 experimental points were obtained and compared with Taitel and Dukler (1976) map as shown in Figure 11. Again, it is observed a good agreement of the experimental data with the map, except for a few intermittent flow points and the dispersed bubble flow in general.

In comparison with the $\alpha = +2.5°$ case, there is not a significant difference in the map lines because of the very small inclination gain.

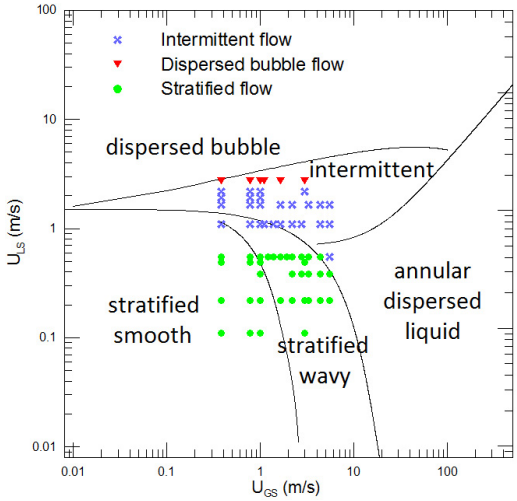

Figure 11. Comparison of the experimental data with Taitel and Dukler (1976) map for downward flow at $5°$.

4.6 $\alpha = +10°$ (downward flow)

For downward flow at $10°$, 28 experimental points were obtained and compared with Taitel and Dukler (1976) map as shown in Figure 12. Again, it is observed a good agreement of the experimental data with the map, except for a few intermittent flow points and, once more, the dispersed bubble flow in general.

It is also important to notice that these small differences between the experimental data and the maps in the tested cases are due to the fact that the transition boundaries should be viewed as transition regions, once the change from one regime to another does not happen in a discontinuous way. Despite these differences, the experimental data appears to follow the curvet's trends.

In comparison to the other downward flow cases, the transition lines difference is more pronounced in terms of increase of the stratified area and reduction of the intermittent area. Even though intermittent flow was observed, it is important to attempt to the fact that all of them were very aerated in a way that bubble nose and tail were not well-shaped.

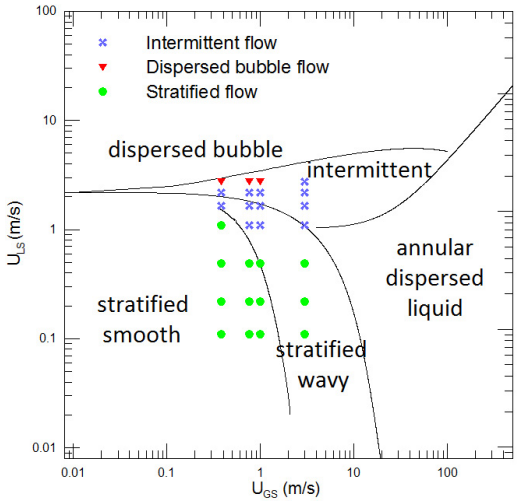

Figure 12. Comparison of the experimental data with Taitel and Dukler (1976) map for downward flow at 10°.

5. CONCLUSIONS

In this study a visualization technique was used to identify two-phase gas-liquid flow regimes in horizontal and slightly inclined air-water flow. Mandhane et al. (1974) and Taitel and Dukler (1976) flow regime maps were implemented in Wolfram *Mathematica 7.0* to generate their maps for horizontal and inclined flow (only Taitel and Dukler (1976)). Then, the experimental data was compared to the obtained maps to check the results and the conclusions deduced were that the visualization technique was able to identify the flow regimes. The Mandhane et al. (1974) experimental map and the Taitel and Dukler (1976) theoretical map have presented a satisfactory agreement with the experimental data.

6. ACKNOWLEDGEMENTS

The authors are grateful to CNPq, CAPES, FAPERJ and CNEN for the financial support received during the realization of this work. Lívia de Oliveira is grateful to CNEN for the undergraduate research scholarship (IC).

7. REFERENCES

Baker, O. (1954). Designing for simultaneous flow oil and gas. *Oil and Gas Journal*, 12:185–195.

Begss, H. D. and Brill, J. P. (1973). A study of two-phase flow in inclined pipes. *Journal of Petroleum Technology*, 25:607–617.

Bui-Dinh, T. and Choi, T. S. (2001). Non-invasive measurements of instantaneous bubble rise velocity using digital image analysis. *Mechanics Research Communications*, 28:471–475.

Fairholm, W. H., Harvel, G. D., Campeau, J. C., and Chang, J. S. (1991). Visualization of two-phase interfaces in natural circulation by real-time neutron radiography. *Proc. Nat. Heat Transfer Conf.*, page 199.

Fossa, M., Guglielmini, G., and Marchitto, A. (2003). Intermittent flow parameters from void fraction. *Flow Measurement and Instrumentation*, 14:161–168.

Govier, G. W. and Aziz, K. (1972). *The Flow of Complex Mixtures in Pipes*. Van Nostrand-Reinhold, New York.

Mandhane, J. M., Gregory, G. A., and Aziz, K. (1974). A flow pattern map for gas-liquid flow in horizontal pipes. *International Journal of Multiphase Flow*, 1:537–553.

Mayor, T. S., Pinto, A. M. F. R., and Campos, J. B. L. M. (2007). An image analysis technique for the study of gas-liquid slug flow along vertical pipes - associated uncertainty. *Flow Measurement and Instrumentation*, 18:139–147.

Mishima, K., Hibiki, T., and Nishihara, H. (1997). Visualization and measurement of two-phase flow by using neutron radiography. *Nuclear Engineering and Design*, 175(1-2):25–35.

Morala, E. C., Cheong, D., Wan, P. T., Irons, G. A., and Chang, J. S. (1984). Ultrasonic wave propagation in a bubbly gas-liquid two-phase flow. *Paper presented at the Multi-Phase Flow and Heat Transfer*, pages 501–512.

Supa-Amornkul, S., Steward, F. R., and Lister, D. H. (2005). Flow visualization study of two-phase flow in the horizontal annulus of the fuel-channel outlet end fitting of a candu reactor. *13th International Conference on Nuclear Engineering - ICONE13*, pages 16–20.

Taitel, Y. and Dukler, A. E. (1976). A model for predicting flow regime transitions in horizontal and near horizontal gas-liquid flow. *Flow Measurement and Instrumentation*, 22:47–55.

Woods, B. D., Fan, Z., and Hanratty, T. J. (2006). Frequency and development of slugs in a horizontal pipe at large liquid flows. *International Journal of Multiphase Flow*, 32:902–925.

Zaruba, A., Krepper, E., Prasser, H. M., and Vanga, B. N. R. (2005). Experimental study on bubble motion in a rectangular bubble column using high-speed video observations. *Flow Measurement and Instrumentation*, 16:277–287.

8. Responsibility notice

The authors are the only responsible for the printed material included in this paper